PERGAMON

International Journal of Heat and Mass Transfer 46 (2003) 1103–1109

International Journal of HEAT and MASS TRANSFER

www.elsevier.com/locate/ijhmt

Contact thermal conductivity of a powder bed in selective laser sintering

A.V. Gusarov [a], T. Laoui [b], L. Froyen [c], V.I. Titov [a,*]

[a] Russian Academy of Sciences, Baikov Institute of Metallurgy, Leninsky Prospect 49, 119991 Moscow, Russia
[b] School of Engineering and the Built Environment, University of Wolverhampton, Wolverhampton WV1 1SB, UK
[c] Department of Metallurgy and Materials Engineering, University of Leuven (K.U. Leuven), Kasteelpark Arenberg 44, 3001 Leuven, Belgium

Received 15 October 2001; received in revised form 25 April 2002

Abstract

Estimation of the temperature field in the powder bed in selective laser sintering process is a key issue for understanding the sintering/binding mechanisms and for optimising the technique. Heat transfer may be strongly affected by formation and growth of necks between particles due to sintering when the contact conductivity becomes predominant in the powder bed effective thermal conductivity. The necks often remain small as compared to the particle size. To calculate the effective contact conductivity of such structures a model of independent small thermal contacts is proposed. The conductivity of the considered cubic-symmetry lattices and the random packing of equal spheres depends on the three structural parameters: the relative density, the coordination number, and the contact size. The present model agrees with the known numerical calculations in the range of contact radius to particle radius ratio below 0.3. The strong dependence on the contact size is qualitatively confirmed by experimental data.

Keywords: Powder bed; Selective laser sintering; Contact thermal conductivity; Coordination number

1. Introduction

Selective laser sintering (SLS) technique consists in depositing successively thin powder layers and heating and sintering/binding the powder particles by a scanning laser beam [1]. Three-dimensional parts of a complex shape can be fabricated by SLS. Flexibility is the main advantage of this process, therefore a number of computer-controlled rapid prototyping machines have been developed based on SLS (see, for example, [1]). One of the disadvantages is that complete powder compaction is rarely achieved [2] and thus a post-treatment is often required. On the other hand, this may be useful in synthesizing porous materials [3].

Free poured (loose) or slightly compacted powders with particle size in the range of several microns to several hundreds microns are typically used for SLS [4,5]. They are characterized by high porosity with initially only point contacts between particles. During laser heating, various sintering and rearrangement mechanisms induce the powder binding and densification [6]. Sintering gives rise to formation and growth of necks between the particles, which are in fact surface contacts. However, the laser-heating time in SLS, which is typically a fraction of a second up to about several seconds, is insufficient for complete material compacting by solid state sintering (requiring usually several hours [7]). With liquid phase sintering mechanism, complete elimination of the porosity is generally not possible because repulsion forces arise between particles at a high fraction of the binding liquid component [6]. As a result, the structure of discrete particles connected by relatively thin necks usually remains during and after SLS treatment as

* Corresponding author. Tel.: +7-095-135-94-26; fax: +7-095-135-86-80.
E-mail address: av.gusarov@relcom.ru (V.I. Titov).

0017-9310/03/$ - see front matter
PII: S0017-9310(02)00370-8

Nomenclature

A	area
a	contact radius
F	heat flux
f	distribution function
n	coordination number
p	relative density
r	radial coordinate
$\overline{r}$	radius-vector
R	particle radius
S	thermal resistance
T	temperature
u	normalized temperature
x	contact size ratio
z	axial coordinate

Greek symbols

ζ, ρ	normalized coordinates
θ	polar angle
λ	thermal conductivity
λ_e	effective thermal conductivity
τ	normalized temperature
φ	heat flux density
$\overline{\Omega}$	unit vector of direction

clearly observed on the scanning electron microscope micrographs [3].

The various types of sintering mechanisms yielding powder binding, depend strongly on temperature [7]. This indicates that calculation of temperature fields in the powder bed in SLS plays a key role in understanding the operating sintering mechanisms (depending on the powder type and process parameters) and in estimating the binding kinetics. However, the associated heat transfer phenomena taking place in SLS process are complex including incident laser radiation penetration into the powder bed, thermal radiation transfer, and thermal conduction through the gas filling the pores and through the contacts between the particles [8,9]. Thermal conductivity of gases at the normal pressure is 3–4 orders lower than that of metals, therefore in a wide range of neck size to particle size ratio, contact conductivity predominates in the powder bed effective thermal conductivity. It becomes more important if sintering is performed in vacuum.

A number of models for evaluating the effective thermal conductivity of composite media containing inclusions embedded in a homogeneous matrix are known, starting with the early work of Maxwell [10]. The Maxwell approach is valid if the inclusions volume fraction or the thermal conductivity difference between inclusions and matrix is low. This model has been extended to take into account high concentration of regularly distributed spherical, cylindrical, and spheroidal inclusions [11–15], inclusions with interfacial thermal resistance [13–15], as well as polydisperse [16] and randomly distributed [17] inclusions. Application of numerical methods allows, in principle, to consider any heterogeneous structure [18].

It should be noted that the above models [10–18] are difficult to apply to powder beds because they do not take into account contacts between particles and high difference in thermal conductivities between a particle and a gas in the pores. Dedicated models for packed beds [19–23] and lattices of overlapped spheres [24,25] have been developed. While some authors paid attention to the gas filling the pores [19,20], other considered the contacts between particles [21–25].

The effective contact conductivity λ_e of the simple cubic (SC) structure of equal overlapped spheres may be estimated using the Reimann–Weber equation [24]:

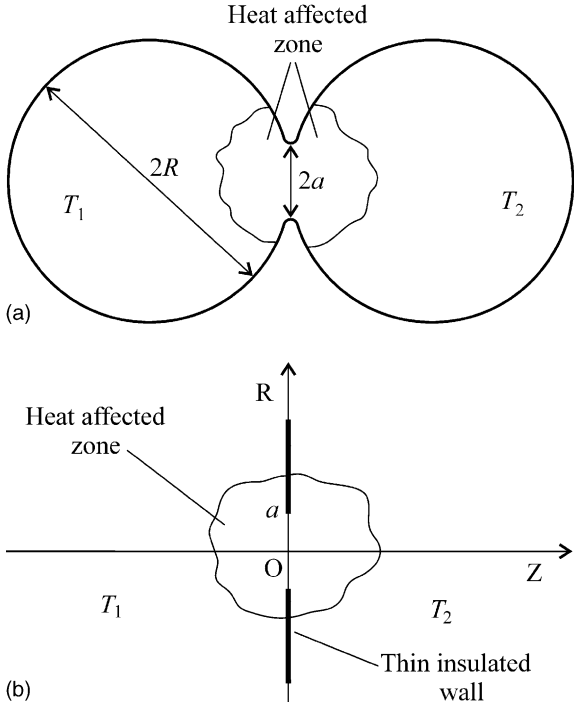

Fig. 1. (a) Contact of radius a between two spherical particles with the same radius R and temperatures T_1 and T_2. (b) Circular contact between two half-infinite insulated bodies: the thin insulated wall simulates the gap between particles where they are not in contact. The lines (OZ) and (OR) denote the axes of the cylindrical frame.

$$\lambda_e = \lambda\left(\frac{1}{x} + \frac{1}{\pi}\ln\frac{2}{x}\right)^{-1}, \quad (1)$$

where λ is the conductivity of dense material in the bulk of a sphere and $x = a/R$ is the contact size ratio, i.e. the ratio of the contact spot radius a to the sphere radius R (see Fig. 1(a)). The face centred cubic (FCC), body centred cubic (BCC), and SC structures of equal spheres with small contacts were considered based on numerical calculation of a temperature field in a single sphere with two surface contacts [21]. Heat transfer between a close-packed structure of equal spheres and a wall was calculated in [23]. A numerical method for calculating periodic lattices was proposed and applied to FCC structure of overlapped spheres [25]. It was shown that the effective conductivity of such a structure considerably differs from the conductivity given by the Maxwell model.

The advantages of numerical methods are evident when the spheres overlap significantly: the contacts influence each other and two contacts may even merge together. However, in the SLS process, the contacts often remain small. The present work addresses such a problem and attempts to find a solution. Simplification are made to allow considering powder beds with a wide range of porosity and coordination number corresponding to various periodic and random structures.

2. Analysis

The scheme of heat transfer between two particles with temperatures T_1 and T_2 is shown in Fig. 1(a). At low neck radius a, a heat affected zone with a high-temperature gradient is formed near the contact, while the temperature in the rest of a particle is almost uniform. The total conductive heat flux through a contact from the particle with temperature T_1 to the one with temperature T_2, is

$$F = (T_1 - T_2)/S, \quad (2)$$

where S is the thermal resistance, which may be estimated at $x \ll 1$ as that of a circular contact between two half-infinite bodies with the thermal conductivity of dense material λ as shown in Fig. 1(b).

The steady-state temperature distribution near the thermal contact may be obtained from the Laplace equation:

$$\frac{\partial^2 T}{\partial z^2} + \frac{1}{r}\frac{\partial}{\partial r}\left(r\frac{\partial T}{\partial r}\right) = 0, \quad (3)$$

where the cylindrical frame is introduced so that z-axis connects the centres of the particles and $z = 0$ corresponds to the contact surface (see Fig. 1(b)). Eq. (3) is to be solved in the infinite domain, $z = -\infty, \ldots, \infty$, $r = 0, \ldots, \infty$, with the boundary condition of the insulated wall in the plane $z = 0$ out off the contact:

$$\frac{\partial T}{\partial z} = 0 \quad \text{at } \{z = 0,\ r > a\}. \quad (4)$$

Conditions at infinity are the following:

$$T \to T_1 \quad \text{at } z \to -\infty \quad \text{and} \quad \text{at } \{r \to \infty,\ z < 0\}, \quad (5)$$

$$T \to T_2 \quad \text{at } z \to \infty \quad \text{and} \quad \text{at } \{r \to \infty,\ z > 0\}. \quad (6)$$

The problem (3)–(6) is anti-symmetric about the plane $z = 0$:

$$T(r,z) + T(r,-z) = T_1 + T_2. \quad (7)$$

This means that over the surface of the contact, where temperature is continuous, it is uniform:

$$T = \frac{T_1 + T_2}{2} \quad \text{at } \{z = 0,\ r < a\}. \quad (8)$$

Taking into account Eq. (7), it is sufficient to solve the Laplace equation (3) in the half-space $z < 0$ with the boundary conditions (4), (5), and (8) or in the half-space $z > 0$ with the boundary conditions (4), (6), and (8).

Each of the two problems is the same one, which arises when one is calculating the electrostatic field of a charged conductive disk, and may be solved by introducing the ellipsoidal frame [26]. Finally, the temperature field of a circular contact is expressed as

$$T = \begin{cases} T_1 + \frac{T_2 - T_1}{2}u(r/a, z/a), & z < 0, \\ T_2 + \frac{T_1 - T_2}{2}u(r/a, z/a), & z \geqslant 0, \end{cases} \quad (9)$$

where the dimensionless function $u(\rho,\zeta)$ of the dimensionless coordinates ρ and ζ is

$$u = \frac{2}{\pi}\arctan\frac{\sqrt{2}}{\sqrt{\rho^2 + \zeta^2 - 1 + \sqrt{(\rho^2 + \zeta^2 - 1)^2 + 4\zeta^2}}}. \quad (10)$$

Temperature distribution (9) is shown in Fig. 2: it is discontinuous at the insulated wall, $\{z = 0,\ r > a\}$. The temperature gradient reaches a maximum at the contact and decreases with the distance to the contact. The temperature tends to the constant left and right values at distances much higher than the contact size. Thermal resistance of a circular contact between two half-infinite bodies with the thermal conductivity λ is derived from (9) as

$$S = \frac{T_2 - T_1}{\lambda\int_0^a \frac{\partial T}{\partial z}\big|_{z=0} 2\pi r\,\mathrm{d}r} = \frac{1}{2\lambda a}. \quad (11)$$

The fact that a contact between two particles disturbs the temperature fields in each of them only in a heat affected zone with the size of the order of several neck sizes may be used in calculating the effective conductivity: at sufficiently small necks the contacts formed between a particle and all the neighbouring particles may be considered as independent. In this case instead

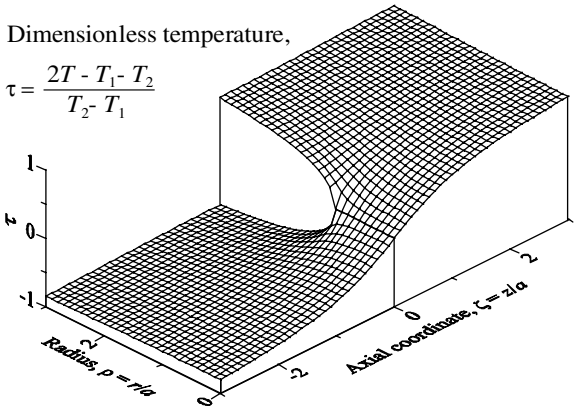

Fig. 2. Temperature distribution, $T(r,z)$, in the heat affected zone of a circular contact between two half-infinite bodies with temperatures of T_1 (left) and T_2 (right): a is the contact radius.

of conventional calculating the temperature field in an elementary cell containing several particles and contacts between them [20–23,25], it is sufficient to take into account configuration of contacts in a given powder structure and to use the thermal resistance of an isolated contact presented by Eq. (11). This approach is justified when the contact size ratio is much less than unity, $x \ll 1$. In practice, the upper bound of x may be estimated comparing the results with the known numerical calculations as presented in Section 4.

3. Results

3.1. Regular structures

Heat flux due to conduction through contacts between particles in a powder bed may be directly obtained in the case of a regular structure. In the systems with cubic symmetry the thermal conductivity tensor reduces to a scalar. So calculating effective thermal conductivity along an arbitrary direction is sufficient.

For example, if spherical particles of equal size are packed in a SC lattice (see Fig. 3) and the gradient of temperature, ∇T, is directed along [1 0 0] axis, the heat flux through the corresponding (1 0 0) plane may be calculated as follows: Temperature difference between the upper and lower monolayers is $\Delta T = T_2 - T_1 = 2R|\nabla T|$. The area of the (1 0 0) plane per one contact between an upper and lower particles is $A = (2R)^2$ Therefore, the effective heat flux density is 1

$$\varphi = \frac{F}{A} = \frac{\Delta T}{SA} = \lambda_e |\nabla T|, \tag{12}$$

where $\lambda_e = \lambda x$ is the effective thermal conductivity of the cubic structure.

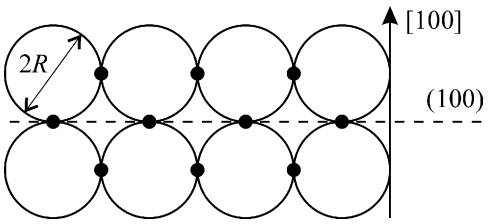

Fig. 3. Cubic structure of particles. Cross-section of two adjacent (1 0 0) monolayers: particles (open circles); contacts (points); (1 0 0) plane (broken line); [1 0 0] direction (arrow).

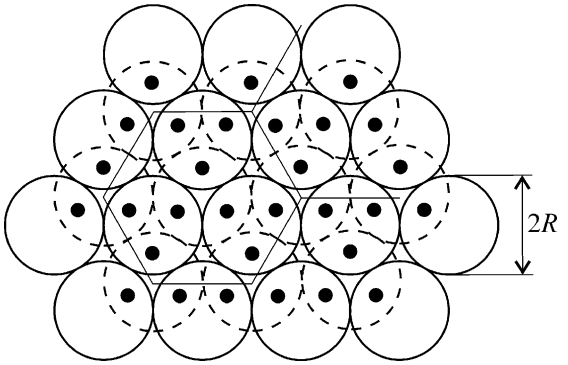

Fig. 4. Close-packed structure of particles. Two adjacent close-packed monolayers: particles of the upper layer (full-line circles) and of the lower one (broken-line circles); contacts between the upper and the lower layers (points).

In close-packed structures, such as the FCC one, effective thermal conductivity in the direction of the normal to a close-packed plane ([1 1 1] FCC) may be obtained from Fig. 4. All the plain may be covered by regular hexagons shown here by thin line. Each hexagon contains 9 contacts and has an area of $3\sqrt{3}R^2$. Hence, the average area per contact is $A = (\sqrt{3}/3)R^2$. The distance between the two layers is $d = (2\sqrt{2}/\sqrt{3})R$ and the increment of temperature is $\Delta T = d|\nabla T|$. Substitution of these expressions into Eq. (12) gives an effective thermal conductivity of $\lambda_e = 2\sqrt{2}\lambda x$.

For particles packed in a diamond-like structure with a gradient of temperature directed along [1 1 1] axis, there are three contacts responsible for heat transfer through each regular hexagon lying in (1 1 1) plain (one of them is shown in Fig. 5). The average area per contact is $A = 16(\sqrt{3}/3)R^2$ and the temperature difference between each of the considered pairs of particles is $\Delta T = 2R|\nabla T|$. Eq. (12) gives then an effective thermal conductivity of $\lambda_e = (\sqrt{3}/4)\lambda x$. The thermal conductivity of regular structures is summarized in Table 1. Both the above-considered problems and the results on the BCC structure are listed there.

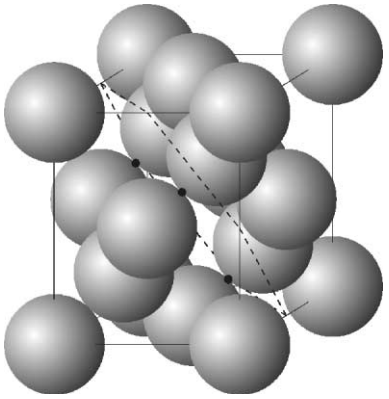

Fig. 5. Diamond-like structure: particles (spheres with radius R); unit cell (thin line cube with the edge of $8(\sqrt{3}/3)R$); plane of (1 1 1) type (broken line); contacts corresponding to heat transfer through the plane (points).

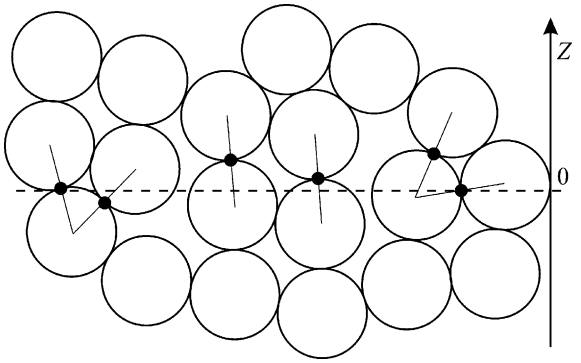

Fig. 6. Heat transfer through necks in the random structure of spherical particles: particles (open circles); contacts between particles (points). Axis Z is directed along the vector of temperature gradient. Only contacts contributing to heat transfer through the marked plane (broken line) are shown. Thin lines link the centres of particles, which take part in the heat transfer through the plane.

Table 1
Effective thermal conductivity of regularly packed equal spheres, λ_e

Structure	p[a]	n[b]	$\lambda_e/(\lambda x)$[c]
FCC	$\pi\sqrt{2}/6 = 0.740$	12	$2\sqrt{2} = 2.828$
BCC	$\pi\sqrt{3}/8 = 0.680$	8	$\sqrt{3} = 1.732$
SC	$\pi/6 = 0.524$	6	1
Diamond	$\pi\sqrt{3}/16 = 0.340$	4	$\sqrt{3}/4 = 0.433$

[a] Relative density.
[b] Coordination number.
[c] Dimensionless thermal conductivity.

3.2. Random structure

Let a contact between two contiguous particles be characterised by its radius-vector $\bar{r}$ taken as the middle of the segment between the centres of the particles, $\bar{r}_1$ and $\bar{r}_2$: $\bar{r} = (\bar{r}_1 + \bar{r}_2)/2$, and the unit vector of direction, $\overline{\Omega} = (\bar{r}_1 - \bar{r}_2)/|\bar{r}_1 - \bar{r}_2|$. The distribution function of contacts, $f(\bar{r}, \overline{\Omega})$, may be introduced so that $f\,\mathrm{d}\bar{r}\,\mathrm{d}\overline{\Omega}$ is the number of contacts inside the element of volume $\mathrm{d}\bar{r}$ and solid angle $\mathrm{d}\overline{\Omega}$. In the uniform isotropic randomly packed structure of spheres with radius R, the distribution is

$$f\,\mathrm{d}\bar{r}\,\mathrm{d}\overline{\Omega} = \frac{1}{2} pn \frac{\mathrm{d}\bar{r}}{(4/3)\pi R^3} \frac{\mathrm{d}\overline{\Omega}}{4\pi}, \tag{13}$$

where p is the relative density, i.e. the ratio of the volume occupied by particles to the total powder bed volume, n the mean coordination number. The factor of $1/2$ in the right-hand side of Eq. (13) takes into account that two opposite values of the direction vector, $\overline{\Omega}$ and $-\overline{\Omega}$, correspond in fact to the same contact.

Conductive heat transfer through the plane $z = 0$, which is normal to the vector of temperature gradient, ∇T (see Fig. 6), may be derived from the distribution function as

$$\varphi = \int_{4\pi} \mathrm{d}\overline{\Omega} \int_{-R\cos\theta}^{R\cos\theta} \frac{\Delta T(\theta)}{S} f\,\mathrm{d}z, \tag{14}$$

where θ is the polar angle. The limits of integration over z and the temperature difference through the contact, $\Delta T(\theta) = 2R\cos\theta|\nabla T|$, are chosen here in assumption that:

(i) the contact between two particles contributes to heat transfer through a surface only if the centres of the particles are on the different sides of the surface;
(ii) the difference in temperature between two neighbouring particles depends on their radius-vectors, $\bar{r}_1$ and $\bar{r}_2$, as

$$\Delta T = T_1 - T_2 = (\bar{r}_1 - \bar{r}_2)\nabla T = 2R\overline{\Omega}\nabla T. \tag{15}$$

Eqs. (11)–(15) give the effective thermal conductivity of a random structure:

$$\frac{\lambda_e}{\lambda} = \frac{pn}{\pi} x. \tag{16}$$

4. Discussion

For the regular structures the effective conductivity is proportional to the contact size but the proportionality factors strongly depend on the structure type (e.g. SC, BCC, FCC, and diamond-like). In general, at a given contact size the conductivity increases with the density and the coordination number (see Table 1). As shown in

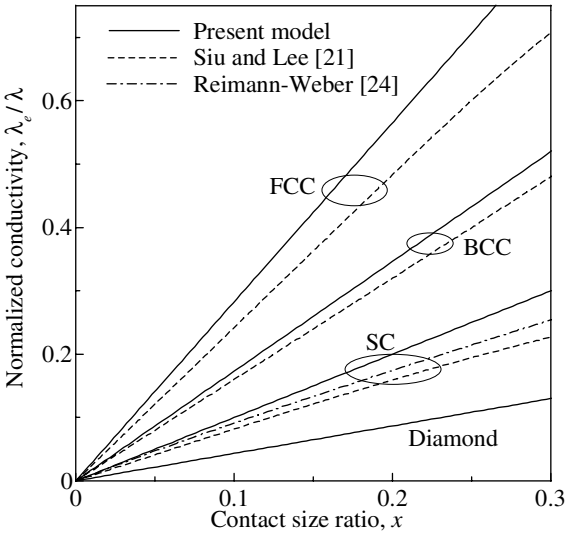

Fig. 7. Effective conductivity of powder bed versus contact size. Comparison between the present model (solid curves) and those of Siu and Lee [21] (broken curves) and Reimann and Weber [24] (chain curve, Eq. (1)) for equal spheres packed in cubic lattices: FCC, BCC, SC, and Diamond-like (marked near the corresponding curves).

Fig. 7, the Reimann–Weber model [24], and numerical calculations of Siu and Lee [21] give slightly nonlinear conductivity dependencies on the contact size x. When x tends to zero, the Reimann–Weber equation (1) provides exactly the same result as the present consideration for the SC lattice. The present model somewhat overestimates the effective conductivity at higher x. However, at least in the range $0 < x < 0.3$ it satisfactorily agrees with the existing models (see Fig. 7).

The proportionality between the effective conductivity and the contact size remains in the case of random packing. Eq. (16) gives an explicit dependence of the proportionality factor on the relative density p and the mean coordination number n. Note that there is no difference in effective conductivity between the considered regular structures with cubic symmetry and random structures with the same values of p and n. This may be easily verified by substituting the values given in Table 1 into Eq. (16). Application of various methods of powder compacting in SLS process gives rise to structures with various density and coordination number, what may considerably influence the effective thermal conductivity according to Eq. (16).

The above theoretical consideration indicates that the effective contact conductivity of powders in SLS process essentially depends on the three structural parameters: the relative density p, the mean coordination number n, and the contact size ratio x. However, in the numerous experimental studies of powder bed thermal conductivity stimulated by the development of the SLS technique (see, for example, [27–29]), the only parameter really taken into consideration was the powder density. Of course, a correlation seems to exist between the coordination number and the density. An example of such a correlation is given by the sequence of regular structures with a wide range of density in Table 1: n increases with p. However, for actual randomly packed powders different coordination numbers are possible for the same density, and thus it is better to treat the two parameters independently from each other.

In the works [29,30] it was pointed out that the effective thermal conductivity of a powder bed might change considerably after a high-temperature heating due to contact area growth during sintering. This qualitatively agrees with our result that the contact effective conductivity is proportional to the contact size. A quantitative experimental study of the contact size impact requires separation of the contact, radiative, and gas contributions to the effective thermal conductivity along with careful structure investigation to estimate the contact size ratio x.

The only essential assumption made in the above theory is the independency of heat transfer through different contacts between particles justified by their small sizes. Therefore, it may be, in principle, extended to take into account polydisperse powders or non-spherical particles. The issue is, however, to describe structures of such powders. This may require further experimental studies or computer simulations.

5. Conclusion

During SLS process, powder beds have usually a structure of discrete particles connected by thin necks. To calculate the effective contact conductivity of such structures a model of independent small thermal contacts is proposed. The conductivity of the considered cubic-symmetry lattices and of the random packing of equal spheres is described by the same equation (Eq. (16)): it depends on the three structural parameters namely the relative density, the mean coordination number, and the contact size. According to the present model, the effective thermal conductivity is proportional to the linear dimension of the contact, which approximately agrees with the existing numerical and analytical models in the range of contact size ratio of $0 < x < 0.3$. The strong dependence on the contact size is qualitatively confirmed by experimental measurements. Application of various methods of powder compacting in SLS process gives rise to structures with various density and coordination number, what considerably influences the effective thermal conductivity.

References

[1] J.-P. Kruth, P. Peeters, T. Smolderen, J. Bonse, T. Laoui, L. Froyen, Comparison between CO_2 and Nd:YAG lasers for use with selective laser sintering of steel-copper powders, Int. J. CAD/CAM Comput. Graphics 13 (1998) 95–110.

[2] N.K. Tolochko, S.E. Mozzharov, I.A. Yadroitsev, V.I. Titov, M.B. Ignatiev, The structure of sintered materials fabricated by a laser beam, Sci. Sintering 31 (1999) 91–96.

[3] H. Yasuda, I. Ohnaka, H. Kaziura, Y. Nishiwaki, Fabrication of metallic porous media by semisolid processing using laser irradiation, Mater. Trans. 42 (2001) 309–315.

[4] J.-P. Kruth, I. Meyvaert, B. Van der Schueren, Powder deposition in selective metal powder sintering, Rapid Prototyping J. 1 (1995) 23–31.

[5] N.K. Tolochko, T. Laoui, L. Froyen, M.B. Ignatiev, V.I. Titov, Fabrication of micromechanical components by laser sintering of fine powders, in: Proceedings of 9 Assises Européennes du Prototypage Rapide and 10 European Conference on Rapid Prototyping and Manufacturing (EURO RP 2001), Paris, France, June 7–8, 2001.

[6] L.A. Anestiev, L. Froyen, Model of primary rearrangement processes at liquid phase sintering and selective laser sintering due to biparticle interactions, J. Appl. Phys. 86 (1999) 4008–4017.

[7] W.D. Kingery, Introduction to Ceramics, Wiley, New York, 1960.

[8] G. Bugeda, M. Cervera, G. Lombera, Numerical prediction of temperature and density distributions in selective laser sintering processes, Rapid Prototyping J. 5 (1999) 21–26.

[9] X.C. Wang, J.-P. Kruth, A simulation model for direct selective laser sintering of metal powders, in: B.H.V. Topping (Ed.), Computational Techniques for Materials, Composites and composite Structures, Civil-Comp, Edinburg, 2000, pp. 57–71.

[10] J.C. Maxwell, A Treatise on Electricity and Magnetism, Dover, New York, 1954.

[11] S.-Y. Lu, Effective conductivities of rectangular arrays of aligned spheroids, J. Appl. Phys. 85 (1999) 264–269.

[12] C. Simovski, S. He, Rapidly convergent expansion method for calculating the effective conductivity of three-dimensional lattices of symmetric inclusions, J. Appl. Phys. 86 (1999) 3773–3779.

[13] G. Gu, Z. Liu, Effects of contact resistance on thermal conductivity of composite media with a periodic structure, J. Phys. D 25 (1992) 249–255.

[14] C.-W. Nan, R. Birringer, D.R. Clarke, H. Gleiter, Effective thermal conductivity of particulate composites with interfacial thermal resistance, J. Appl. Phys. 81 (1997) 6692–6699.

[15] S. Mercier, A. Molinari, M. El Mouden, Thermal conductivity of composite material with coated inclusions: applications to tetragonal array of spheroids, J. Appl. Phys. 87 (2000) 3511–3519.

[16] G.Q. Gu, K.W. Yu, Thermal conductivity of polydisperse composites with periodic microstructures, J. Phys. D 30 (1997) 1523–1530.

[17] M. Grigoriu, Estimation of effective conductivity of random heterogeneous media by diffusion processes, J. Appl. Phys. 82 (1997) 4346–4349.

[18] S. Torquato, I.C. Kim, D. Cule, Effective conductivity, dielectric constant, and diffusion coefficient of digitized composite media via first-passage-time equations, J. Appl. Phys. 85 (1999) 1560–1571.

[19] S. Yagi, D. Kunii, Studies on effective thermal conductivities in packed beds, J. AIChE 3 (1957) 373–381.

[20] A.J. Slavin, F.A. Londry, J. Harrison, A new model for the effective thermal conductivity of packed beds of solid spheroids: alumina in helium between 100 and 500 °C, Int. J. Heat Mass Transfer 43 (2000) 2059–2073.

[21] W.W.M. Siu, S.H.-K. Lee, Effective conductivity computation of a packed bed using constriction resistance and contact angle effects, Int. J. Heat Mass Transfer 43 (2000) 3917–3924.

[22] X.-J. Hu, J.-H. Du, S.-Y. Lei, B.-X. Wang, A model for the thermal conductivity of unconsolidated porous media based on capillary pressure-saturation relation, Int. J. Heat Mass Transfer 44 (2001) 247–251.

[23] S. Kikuchi, Numerical analysis model for thermal conductivities of packed beds with high solid-to-gas conductivity ratio, Int. J. Heat Mass Transfer 44 (2001) 1213–1221.

[24] A.V. Luikov, Heat and Mass Transfer, Handbook, Energia, Moscow, 1971.

[25] J.D. Albrecht, P.A. Knipp, T.L. Reinecke, Thermal conductivity of opals and related composites, Phys. Rev. B 63 (2001) 134303.

[26] L.D. Landau, E.M. Lifschitz, Electrodynamics of Continuum Media, Pergamon, Oxford, 1960.

[27] S.S. Sih, The thermal and optical properties of powders in selective laser sintering, Ph.D. Thesis, University of Texas at Austin, 1996.

[28] I.V. Shishkovskii, N.L. Kupriyanov, Thermal fields in metal-polymer powder compositions during laser treatment, High Temp. 35 (1997) 710–714.

[29] C.M. Taylor, T.H.C. Childs, Thermal experiments in direct metal laser sintering, in: Proceedings of 9 Assises Européennes du Prototypage Rapide and 10 European Conference on Rapid Prototyping and Manufacturing (EURO RP 2001), Paris, France, June 7–8, 2001.

[30] I. Fedina, E. Litovsky, M. Shapiro, A. Shavit, Thermal conductivity of packed beds of refractory particles: Experimental results, J. Am. Ceram. Soc. 80 (1997) 2100–2108.